ARTICLES

Formation of Three C_4H_3N Isomers from the Reaction of CN ($X^2\Sigma^+$) with Allene, H_2CCCH_2 (X^1A_1), and Methylacetylene, CH_3CCH (X^1A_1): A Combined Crossed Beam and Ab Initio Study

N. Balucani,[†,‡] O. Asvany,[†] R.-I. Kaiser,*[,†,§] and Y. Osamura[||]

Institute of Atomic and Molecular Sciences, 1, Section 4, Roosevelt Road, 107 Taipei, Taiwan, ROC, and Department of Chemistry, Rikkyo University, 3-34-1 Nishi-ikebukuro, Toshima-ku, Tokyo, 171-8501, Japan

Received: April 26, 2001; In Final Form: February 8, 2002

Crossed molecular beam reactions of cyano radicals, CN ($X^2\Sigma^+$), with two C_3H_4 isomers—methylacetylene, CH_3CCH (X^1A_1), and allene, H_2CCCH_2 (X^1A_1)—have been investigated at six collision energies between 13.4 and 36.7 kJ mol^{-1} to elucidate the chemical reaction dynamics to form three C_4H_3N isomers—1-cyanomethylacetylene, CH_3CCCN (X^1A_1), cyanoallene, $H_2CCCH(CN)$ (X^1A'), and 3-cyanomethylacetylene, $CH_2(CN)CCH$ (X^1A')—under single collision conditions. The forward-convolution fitting of the laboratory angular and time-of-flight distributions combined with ab initio calculations reveal that both reactions have no entrance barrier, proceed via indirect (complex-forming) reaction dynamics, and are initiated by addition of CN($X^2\Sigma^+$) to the π electron density of the unsaturated hydrocarbon at the terminal carbon atom to form long-lived $CH_3CCH(CN)$ (methylacetylene reaction) and $H_2CCCH_2(CN)$ (allene reaction) intermediates. Both complexes fragment via exit transition states located 8−19 kJ mol^{-1} above the products to form 1-cyanomethylacetylene, CH_3CCCN (X^1A_1), cyanoallene, $H_2CCCHCN$ (X^1A'), and 3-cyanomethylacetylene, $CH_2(CN)CCH$ (X^1A'). Because both reactions are barrierless and exothermic and the exit transition states lie below the energy of the separated reactants, all hydrogen-deficient nitriles identified in our investigation can be synthesized in the atmosphere of Saturn's moon Titan and in molecular clouds holding temperatures as low as 10 K.

I. Introduction

Gas-phase cyano radical, CN($X^2\Sigma^+$), reactions occur in a wide variety of chemical environments such as flames, gas lasers, and planetary atmospheres.[1] In particular, binary collisions of CN with unsaturated hydrocarbons are of great relevance in astrochemistry. Indeed, since the first detection of cyanoacetylene in the interstellar medium, it has been suggested that bimolecular neutral−neutral reactions of the cyano radical with acetylene could be the source of cyanoacetylene in the outflow of circumstellar envelopes surroundings carbon stars, in hot molecular cores, and in dark molecular clouds.[1]

Because of their interest, the reactions of CN radicals with several unsaturated hydrocarbons have been recently investigated with the most sophisticated kinetic techniques, and rate constants have been determined over a broad temperature range. For instance, the reactions with acetylene, methylacetylene, and ethylene were studied down to temperatures as low as 13 K; all of them were found to be very fast and were characterized by rate constants on the order of gas kinetics ($\sim 10^{-10}$ cm^3 s^{-1}).[2] Because these investigations monitor only the decay kinetics of the free radical and do not identify the reaction products, in our laboratory a systematic investigation of CN reactions was engaged by means of the crossed molecular beam method with mass spectrometric detection. The aim has been to determine the primary reaction products and to elucidate the underlying chemical reaction dynamics. Reports on the reaction of CN radicals with acetylene,[3] benzene,[4] dimethylacetylene,[5] and ethylene[6] have already appeared, and a preliminary account of the first experimental results on the reaction CN + CH_3CCH has been given as well.[7] Also, several reviews,[8,9] where the similarities and differences along the series of the investigated CN reactions are noted, have recently appeared. In those reviews, a brief description of the results on the last reaction investigated in our laboratory, namely, CN + CH_2CCH_2, was also included. In all these articles, with the help of ab initio electronic structure calculations that were performed ad hoc, we have presented a detailed picture of all the mentioned reactions.[3−6] Ab initio calculations relative only to the minimum energy path were instead presented in the case of the two isomeric reactions CN + CH_3CCH/CN + CH_2CCH_2.[7−9]

In this article, we present a full account of the experimental results for these two isomeric systems—we investigated each of them at three different collision energies—and we thoroughly report the electronic structure calculations on the common doublet C_4H_3N potential energy surface. Finally, similarities and

* Corresponding author. Email: rik1@york.ac.uk.
† Institute of Atomic and Molecular Sciences.
|| Rikkyo University.
‡ Visiting scientist. Permanent address: Dipartimento di Chimica, Università di Perugia, 06123 Perugia, Italy.
§ Present address: Department of Chemistry, University of York, York YO10 5DD, U.K.

10.1021/jp0116104 CCC: $22.00
Published on Web 04/09/2002

TABLE 1: Experimental Beam Conditions and 1σ Errors—Most Probable Velocity v_p, Speed Ratio S, Most Probable Collision Energy of the CN Beam with C_3H_4 Molecules E_c, and Center-of-Mass Angles, Θ_{CM}

experiment	v_p, m s^{-1}	S	E_c, kJ mol^{-1}	Θ_{CM}
CN/CH_3CCH	1000 ± 50	8.4 ± 0.1	13.4 ± 1.0	52.3 ± 1.7
CN/CH_3CCH	1560 ± 30	6.8 ± 0.5	24.7 ± 0.9	39.6 ± 0.8
CN/CH_3CCH	1930 ± 20	5.1 ± 0.5	34.9 ± 0.6	33.8 ± 0.6
CN/H_2CCCH_2	1460 ± 20	5.5 ± 0.2	22.4 ± 0.5	41.5 ± 0.7
CN/H_2CCCH_2	1850 ± 20	4.5 ± 0.3	32.5 ± 0.7	34.9 ± 0.6
CN/H_2CCCH_2	1990 ± 30	4.5 ± 0.4	36.7 ± 0.9	33.0 ± 0.7
H_2CCCH_2	840 ± 10	8.2 ± 0.2		
CH_3CCH	840 ± 10	8.9 ± 0.2		

discrepancies with the isoelectronic reaction of the d_1-ethynyl radical, C_2D ($X^2\Sigma^+$), with methylacetylene[10] are discussed.

II. Experimental and Data Analyses

All the experiments were performed by employing the 35″ crossed molecular beam machine described in detail elsewhere.[9a,11] A pulsed supersonic cyano radical beam, CN($X^2\Sigma^+$), in the ground vibrational state is generated in situ via laser ablation of graphite at 266 nm and subsequent reaction of the ablated species with neat nitrogen gas that also acts as seeding gas. A chopper wheel located after the ablation source was made to select a 9-μs segment of the broad CN beam so that different velocities can be easily achieved[12] (see Table 1). The pulsed beam intersects the second pulsed hydrocarbon beam (CH_3CCH or H_2CCCH_2) with a crossing angle of 90°. In addition, one set of experiments was performed by replacing CH_3CCH with CD_3-CCH, with the aim of investigating the acetylenic hydrogen versus the methylic deuterium loss channel. Reactively scattered species were monitored using a triply differentially pumped detector consisting of a Brink-type electron-impact ionizer, quadrupole mass filter, and a Daly ion detector. Product velocity distributions were recorded by measuring TOF at different laboratory angles. In the case of the CD_3CCH experiments, TOF spectra were taken only at the center-of-mass angle. Data accumulation times range up to 5 h at each angle. Laboratory angular distributions are then obtained by integrating the TOF spectra at different laboratory angles. Information on the reaction dynamics is obtained by moving from the laboratory (LAB) coordinate system to the center-of-mass (CM) frame and analyzing the CM product angular, $T(\theta)$, and translational-energy, $P(E_T)$, distributions.

III. Electronic Structure Calculations

The potential energy surfaces (PESs) of the reactions of the C_3H_4 isomers with the cyano radical have been examined in terms of ab initio molecular orbital methods. We have employed the hybrid density functional B3LYP method (i.e., Becke's three-parameter nonlocal exchange functional[13] with the nonlocal correlation functional of Lee, Yang, and Parr[14] and the 6-311G-(d,p) basis set[15]). All computations have been carried out using the Gaussian 98 program package.[16] The structures of the intermediates and transition states have been confirmed with vibrational analysis; all relative energies shown in this article are the corrected values of the zero-point vibrational energies. The coupled cluster CCSD(T) calculations with the 6-311G-(d,p) basis set have also been performed for some of the critical structures to refine the energetics.[17]

IV. Results

A. Laboratory Angular and TOF Distributions. For both of the reactions with methylacetylene and allene, the reactive

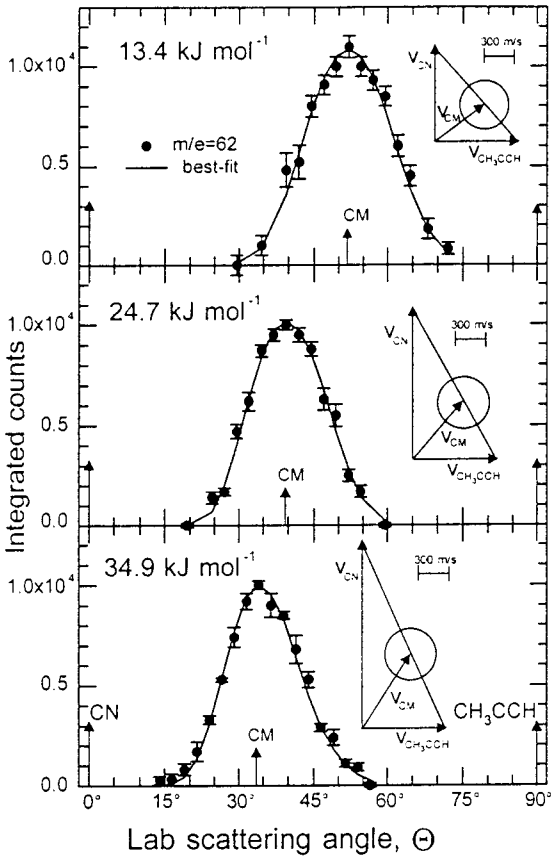

Figure 1. Laboratory angular distributions of the C_4H_3N product measured at $m/e = 62$ at the three collision energies investigated for the CN + CH_3CCH reaction. Dots and error bars indicate experimental data, and the solid lines, the calculated distribution with the best-fit center-of-mass functions. The Newton diagrams showing the kinematics of the experiments are drawn in the top right corner (see text).

scattering signal was detected at $m/e = 65$ ($C_4NH_3^+$), 64 ($C_4NH_2^+$), 63 (C_4NH^+), and 62 (C_4N^+). At each collision energy, TOF spectra revealed identical patterns at all mass-to-charge ratios and could be fit with identical $T(\theta)$ and $P(E_T)$ distributions, which suggests that C_4NH_3 is the only product in this range of masses and that the signal at the lower m/e value results from dissociative ionization. Mass-to-charge ratios higher than 65 were not observed. When using the isotopically labeled CD_3-CCH, we observed a signal at both $m/e = 68$ ($C_4D_3N^+$; H atom loss) and at $m/e = 67$ ($C_4D_2NH^+$; D atom loss). By integration of the TOF spectra at $m/e = 68$ and 67 and by correcting for the mass combination of the products, we derived a branching ratio of the D atom versus the H atom loss channel of ~1.

All the final measurements were taken at $m/e = 62$ because it had the most favorable signal-to-noise ratio. In Figures 1 and 2, the LAB angular distributions at three different collision energies are reported for the two title reactions. The LAB angular distributions for CN + CH_3CCH at $E_c = 24.7$ kJ mol^{-1} and for CN + CH_2CCH_2 at $E_c = 22.4$ kJ mol^{-1} have already been shown.[7-9] We have reported them here to show possible trends with the collision energy. As it is well-visible in Figures 1 and 2, all the LAB angular distributions were found to peak at the CM position angles and depict about the same intensity in the backward and forward directions. All of them are quite broad, extending for ~40° in the scattering plane. The limiting circles reported in the Newton diagrams have been drawn assuming that all the available energy is channeled into the product translational energy, in the case that the most exothermic C_4H_3N isomer is formed in both reactions, that is,

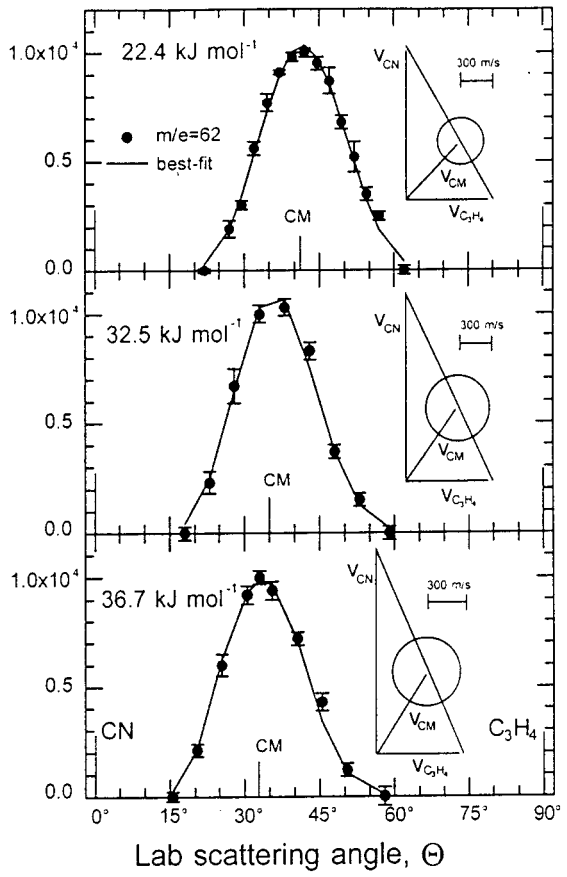

Figure 2. Laboratory angular distributions of the C_4H_3N product measured at $m/e = 62$ at the three collision energies investigated for the CN + CH_2CCH_2 reaction. Dots and error bars indicate experimental data, and the solid lines, the calculated distribution with the best-fit center-of-mass functions. The Newton diagrams showing the kinematics of the experiments are drawn in the top right corner (see text).

1-methylcyanoacetylene (from the methylacetylene reaction) and cyanoallene (from the allene reaction). If these limits are compared with the experimentally determined scattering ranges, then the substantial coincidence of the angular ranges indicates that 1-methylcyanoacetylene and cyanoallene are significantly formed from CN + CH_3CCH and CN + H_2CCCH_2, respectively. Selected TOF spectra are shown in Figures 3 and 4 for CN + CH_3CCH at E_c=13.4 kJ mol^{-1} and CN + CH_2CCH_2 at E_c=32.5 kJ mol^{-1}, respectively. They well-illustrate the main characteristics of the recorded spectra so that results for the other energies are not shown here. The interested reader can find the TOF spectra for CN + CH_3CCH at E_c = 24.7 kJ mol^{-1} and for CN + CH_2CCH_2 at E_c = 22.4 kJ mol^{-1} in refs 7−9. At each collision energy, our experimental data were fit using a single CM angular distribution and a single CM translational-energy distribution.

B. Best Center-of-Mass Functions. Figures 5a and 6a show the CM translational-energy distributions for the two reactions at each E_c investigated. For each set of data, two curves are given that delimit the range of functions that allow a good fit of the experimental data. For both reactive systems, the $P(E_T)$'s peak well away from zero translational energy. However, in the case of the CN + CH_3CCH reaction, the maximum is located between 15 and 30 kJ mol^{-1}, whereas the peak is more rounded and shifts to larger energies of 27−50 kJ mol^{-1} in the case of CN + CH_2CCH_2 reaction. This difference is somewhat significant and suggests that the exit transition state(s) from the decomposing intermediate(s) to the product(s) is (are) tighter

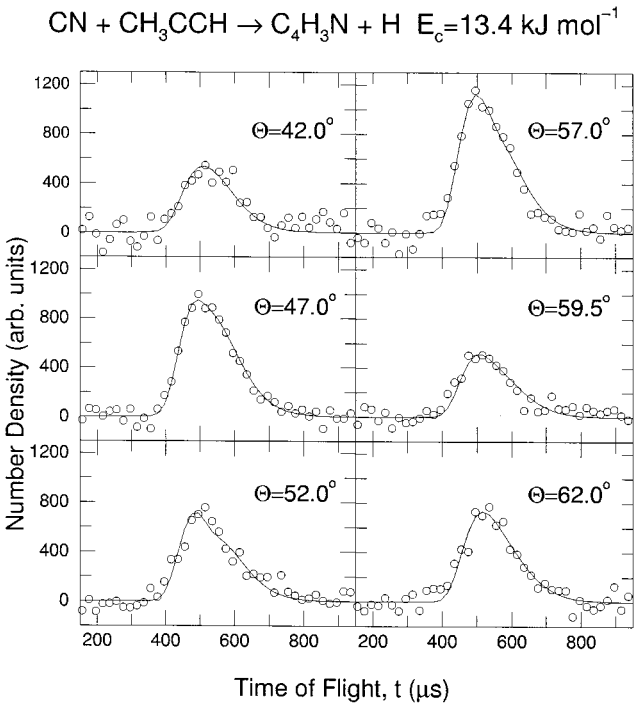

Figure 3. Selected TOF spectra ($m/e = 62$) at distinct laboratory angles for the CN + CH_3CCH reaction at a collision energy of 13.4 kJ mol^{-1}. The circles represent the experimental data, and the solid lines, the calculated fit.

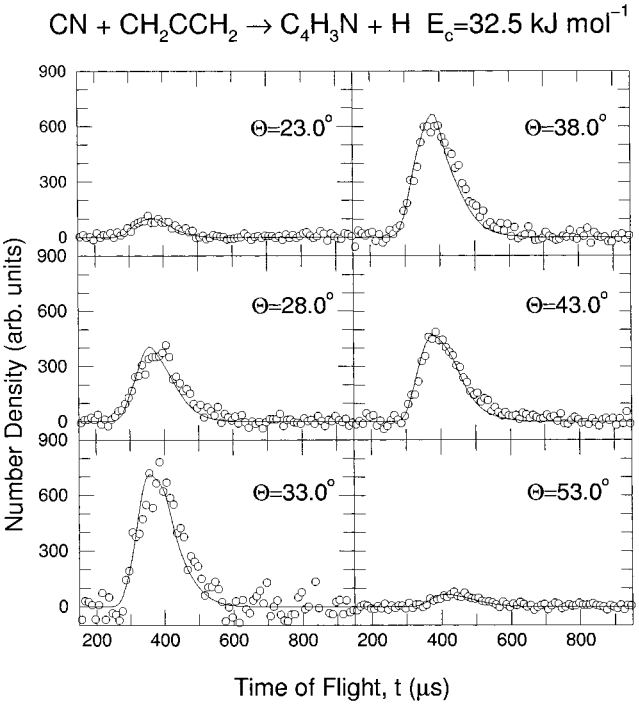

Figure 4. Selected TOF spectra ($m/e = 62$) at distinct laboratory angles for the CN + CH_2CCH_2 reaction at a collision energy of 32.5 kJ mol^{-1}. The circles represent the experimental data, and the solid lines, the calculated fit.

for the CN/allene system than it is for CN/methylacetylene. The maximum value reached by the $P(E_T)$'s is found to be between 80 and 130 kJ mol^{-1}, 90 and 135 kJ mol^{-1}, or 90 and 140 kJ mol^{-1} for the methylacetylene reaction (from the lowest to the highest collision energy) and between 95 and 105 kJ mol^{-1}, 100 and 110 kJ mol^{-1}, or 120 and 130 kJ mol^{-1} for the allene reaction (from the lowest to the highest collision energy). If

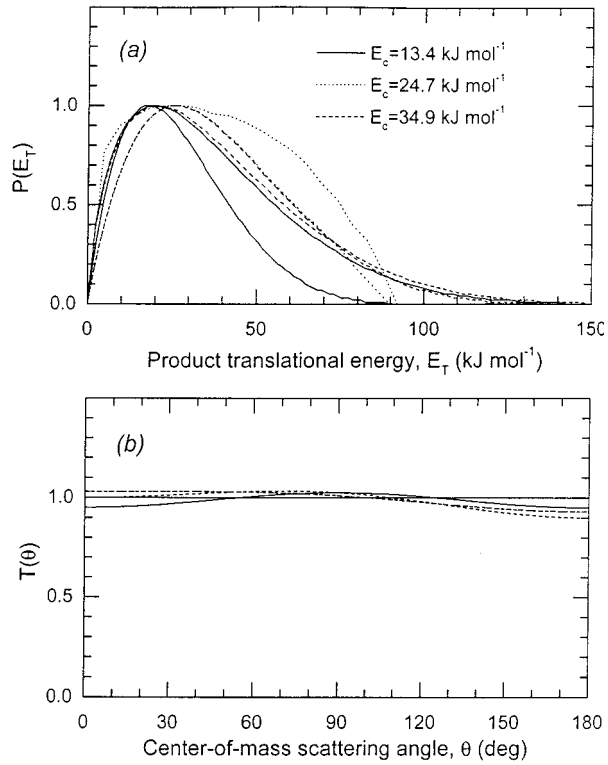

Figure 5. Center-of-mass translational energy (a) and angular flux (b) distributions for the reaction $CN(X^2\Sigma^+) + CH_3CCH \rightarrow C_4H_3CN + H(^2S_{1/2})$ at the different collision energies.

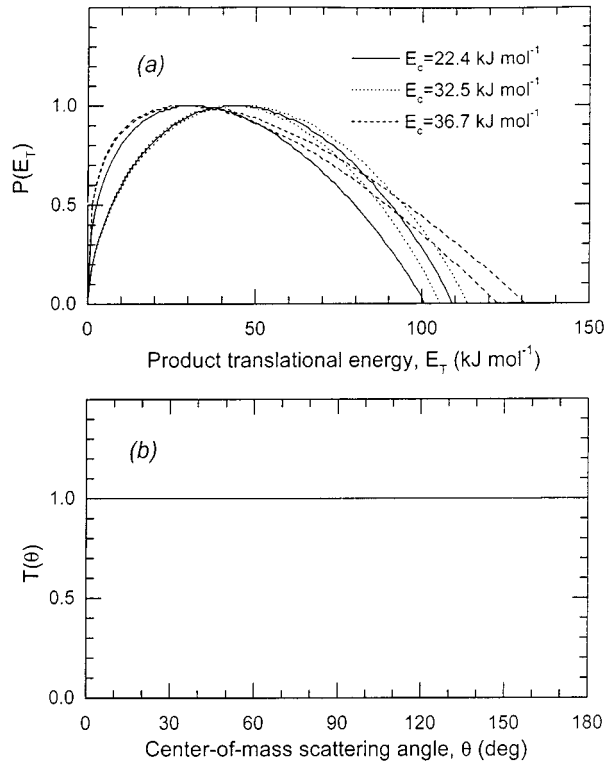

Figure 6. Center-of-mass translational energy (a) and angular flux (b) distributions for the reaction $CN(X^2\Sigma^+) + CH_3CCH \rightarrow C_4H_3CN + H(^2S_{1/2})$ at the different collision energies.

we subtract the relative collision energies, the CN/H exchange reactions turn out to be exothermic by about 65−115 kJ mol^{-1} (methylacetylene) and 73−94 kJ mol^{-1} (allene). This finding nicely agrees with the reaction enthalpies derived from our electronic structure calculations relative to the most exothermic channel in the two cases (see below). In fact, the reaction to form 1-cyanomethylacetylene is calculated to be exothermic by 106 kJ mol^{-1} for CN + CH_3CCH, whereas the reaction exothermicity to form the cyanoallene isomer in the case of CN + CH_2CCH_2 is calculated to be 86 kJ mol^{-1}. Finally, the average energy released into the translational degrees of freedom is found to be 30−40 kJ mol^{-1} (∼30% of the total available energy) and 40−50 kJ mol^{-1} (∼40% of the total available energy) for the methylacetylene and allene reactants, respectively. Again, the larger kinetic energy release for the allene reaction might be attributed to a tighter exit transition state to the products and hence a more repulsive bond rupture as compared to that of the methylacetylene system.

The CM angular distributions, $T(\theta)$, of the cyano radical reactions with the allene molecule are forward−backward symmetric and isotropic at all collision energies (see Figure 6b). An identical shape was found at the lowest collision energy of the methylacetylene system (see Figure 5b). An isotropic distribution is backward−forward symmetric and therefore implies either a lifetime of the decomposing complex(es) that is longer than its rotational period or a "symmetric-exit transition state". In the latter case, the rotation should interconvert the leaving hydrogen atom in the decomposing complex via a proper rotation axis, with the consequence that the complex would fragment with equal probability along the direction defined by θ or $\pi - \theta$, which would result in a symmetric flux distribution, even in the case that the lifetime of the complex might be less than a rotational period.[18] Because the electronic structure calculations depict no symmetric-exit transition state(s) (see below), we conclude that the lifetime of the intermediate(s) is longer than its (their) rotational period(s). At the higher collision energies of 24.7 and 34.9 kJ mol^{-1} of the CN + CH_3CCH reaction, best fits of our data were achieved with slightly forward-scattered $T(\theta)$ values with intensity ratios of $I(180°)/I(0°) \approx 0.9$ (see Figure 5b). In any case, all six $T(\theta)$ values show intensities over the whole angular range between 0° and 180°, demonstrating that both reactions follows indirect scattering dynamics via C_4H_4N complex(es). The absence of polarization in the $T(\theta)$s might well result from poor coupling between the initial L and the final orbital angular momentum value L′, indicating that most of the total angular momentum channels into rotational excitation of the heavy product(s).

V. Discussion

A. Ab Initio C_4H_4N Potential Energy Surface. In the following section, we report the results of a computational investigation of the interaction of the cyano radical, $CN(X^2\Sigma^+)$, with the methylacetylene and allene molecules. The discussion is limited to the formation of the nitrile isomers; previous calculations revealed that the formation of isonitriles in both systems is endothermic by 8−14 kJ mol^{-1}.[8] Considering the involved exit barriers of 10−15 kJ mol^{-1}, isonitriles are predicted to be only a minor reaction product (<2−4%), if any, in our crossed-beam experiments at the highest collision energies.

We begin by discussing the reaction CN + CH_3CCH. According to our ab initio calculations, CN can attack the π orbital of the methylacetylene molecule at the C1 position, with the radical center located on the $^2\Sigma^+$ orbital of the carbon atom. This approach is barrierless and forms the deeply bound (253 and 252 kJ mol^{-1}) **INT1a** collision complex that can isomerize to **INT1b** via small barriers of only 17 and 16 kJ mol^{-1} through **TS1x** on the $^2A'$ surface (cf. Figures 7−8). An alternative

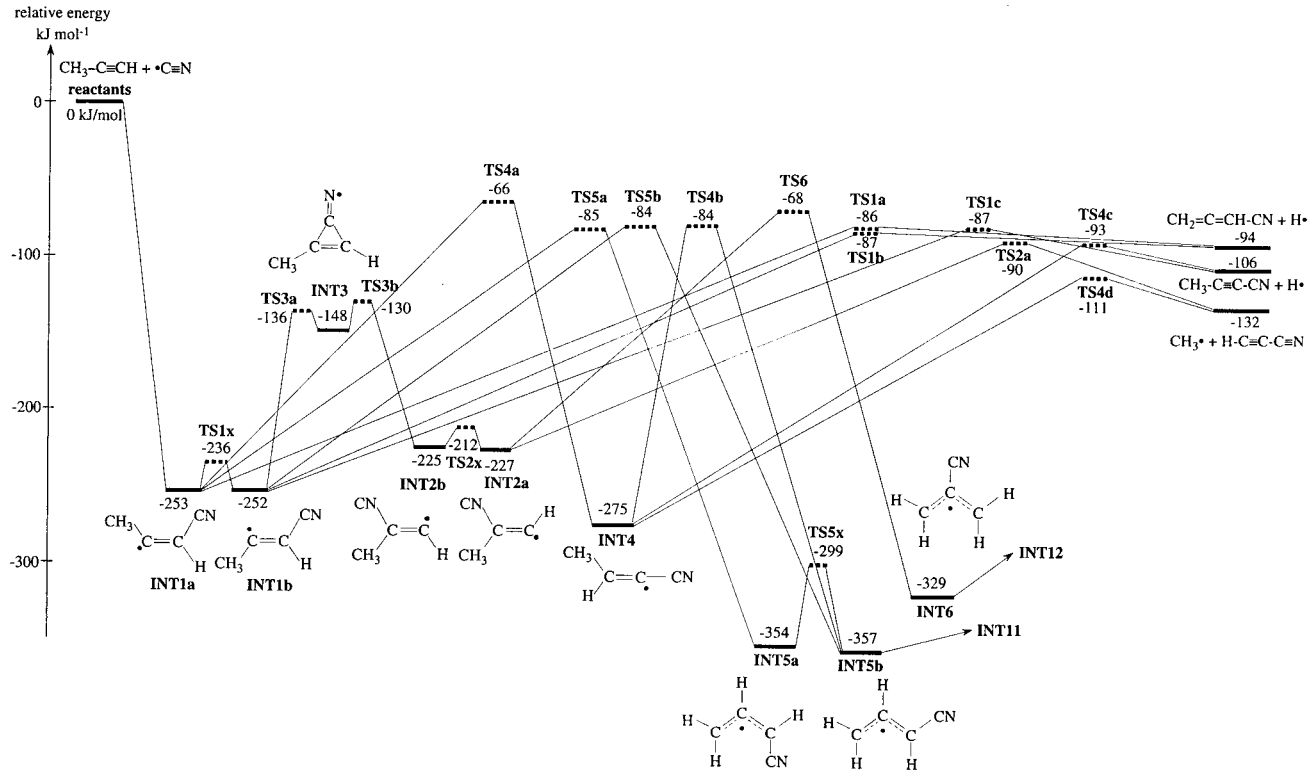

Figure 7. Schematic representation of the C_4H_3N potential energy surface of the CN + CH_3CCH reaction. Only the most likely initial addition pathway is shown (see text).

addition of the cyano radical to the C2 atom of the methylacetylene unit could lead to **INT2a** and **INT2b**. Similar to that of **INT1a/b**, cis−trans isomerization involves only minor barriers of 13 and 15 kJ mol^{-1} through **TS2x**. However, compared to that of **INT1a/b**, these intermediates are less stable and are bound only by 225 and 227 kJ mol^{-1}. This destabilization is the effect of the energetically unfavorable repulsion of the cyano and methyl groups in **INT2a/b**. All isomers discussed so far are doublet radicals and have C_s symmetry. The cis isomers **INT1b** and **INT2b** can isomerize through a three-membered cyclic intermediate **INT3** via a migration of the cyano group from C1 to C2 and vice versa. This intermediate is loosely bound by only 148 kJ mol^{-1} with respect to the energy of the separated reactants; the low-lying transition states **TS3a** and **TS3b** located only 12 and 18 kJ mol^{-1}, respectively, above **INT3** connect it to **INT1b** and **INT2b**, respectively.

The initial addition complexes can react via (a) H atom elimination, (b) methyl group loss, or (c) hydrogen migration. A hydrogen atom in **INT1a/b** can be ejected from C1 or from the methyl group adjacent to C2 to form either the 1-cyanomethylacetylene isomer CH_3CCCN via **TS1c** or the cyanoallene molecule through **TS1a/b**. All transition states are similar in energy within 1 kJ mol^{-1}. The decay to 1-cyanomethylacetylene involves a tighter exit transition state of 19 kJ mol^{-1} compared to that of the fragmentation yielding the cyanoallene isomer via the relatively loose, productlike transition states **TS1a/b** located 8 and 7 kJ mol^{-1}, respectively, above the reaction products. The overall reactions to form 1-cyanoacetylene and cyanoallene were found to be exothermic by 106 and 94 kJ mol^{-1}, respectively. A potential H atom elimination from **INT2a/b** at the C1 position yields a singlet carbene isomer CC(CN)(CH_3). Because the overall reaction to yield this structure is endothermic by 129.0 kJ mol^{-1}, this pathway is closed in our experiments, considering the highest collision energy of 34.9 kJ mol^{-1}. We consider now the methyl group-loss pathway. Here, a methyl group ejection from **INT1a/b** forms a carbene structure CC(CN)H. Because the reaction is endothermic by 77.0 kJ mol^{-1}, this singlet carbene plays no role in the chemical reaction dynamics of the title reactions. However, a CH_3 group loss from **INT2a** via **TS2a** yielding cyanoacetylene is energetically feasible.

Finally, **INT1a** can undergo a 1,2 H shift to form the **INT4** isomer (C_s point group), which is energetically favored by 22 kJ mol^{-1} compared to **INT1a**. The energetics of the transition state **TS4a** of 187 kJ mol^{-1} with respect to the energetics of **INT1a** are of the same order of magnitude compared to those of other hydrogen shifts, as found in the initial addition complexes of cyano radical reactions with acetylene (177 kJ mol^{-1})[3] and ethylene (136 kJ mol^{-1}).[4] **INT4** either ejects a methyl group via **TS4d** to form cyanoacetylene or a hydrogen atom to form 1-cyanomethylacetylene via **TS4c**. Both intermediates **INT4** and **INT2a** could show further hydrogen atom migrations from the methyl group to C1 via **TS4b** and **TS6** to **INT5b** and **INT6**, respectively. Both latter structures are more stable than **INT1-4** and reside in deep potential energy wells of 357 and 329 kJ mol^{-1}, respectively. This enhanced stabilization can be rationalized in terms of the resonance stabilization of the free radicals, as **INT6** and **INT5b** represent 1- and 2-substituted cyanoallyl radicals. **INT5b** can react to form **INT5a** via a cis/trans isomerization (**TS5x**). An alternative route to **INT5a/b** involves 3,2 H shifts in **INT1a** and **INT1b** via **TS5a** and **TS5b**, respectively.

Both **INT5b** and **INT6** are very interesting and connect the C_4H_3N PES of the CN + CH_3CCH reaction with that of CN + CH_2CCH_2 (cf. Figures 9 and 10). Here, the potential energy surface for the initial addition of the cyano radical to terminal and central carbon atoms of the allene molecule indicates the attractiveness of forming **INT7a/b** and **INT6**, respectively, without entrance barriers. The cis and trans isomers **INT7a** and **INT7b**, respectively, can be interconverted via a low-lying

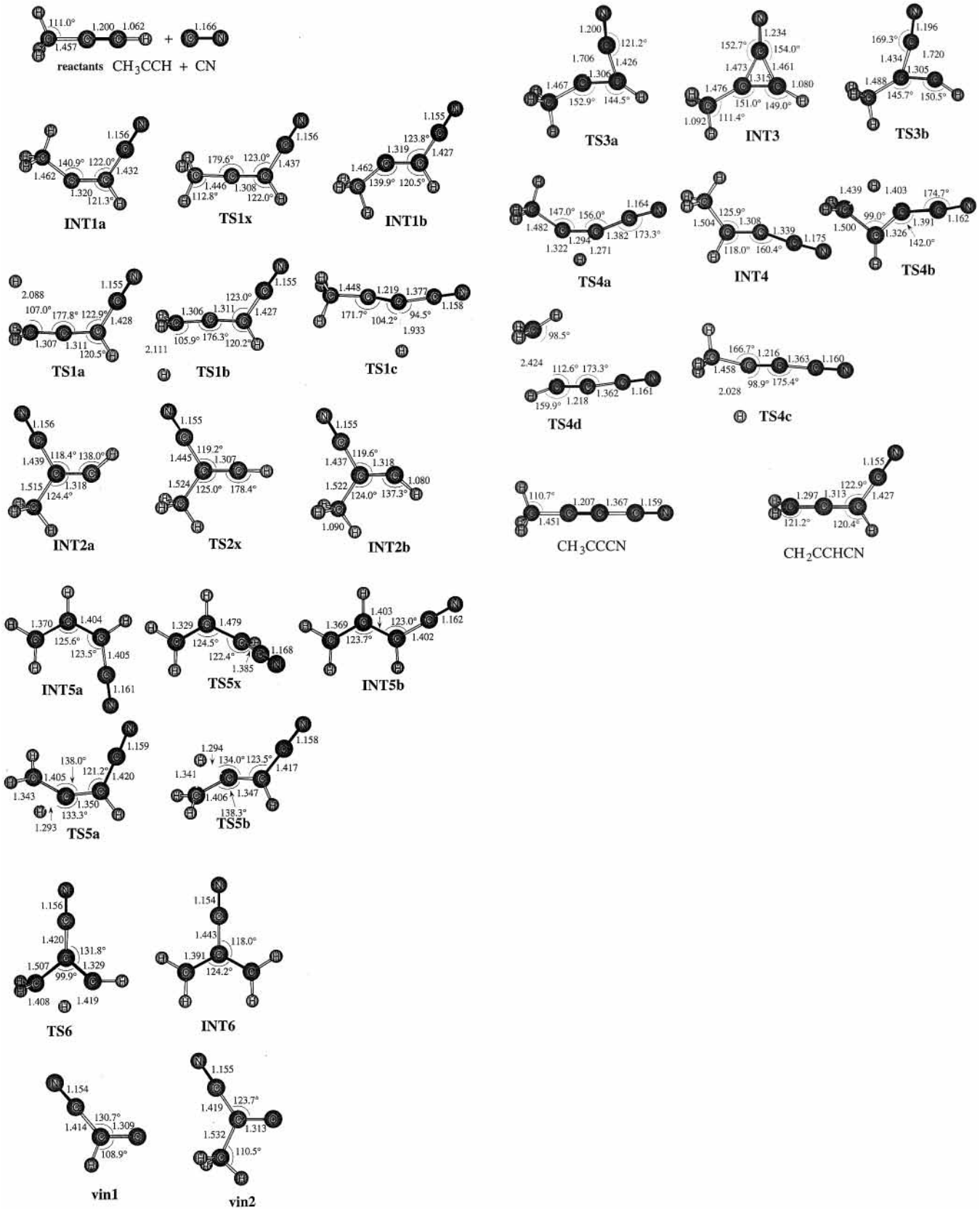

Figure 8. Important bond distances (Å) and bond angles (deg) of reactants, intermediates, transition states, and products of Figure 7.

transition state **TS7x** and hence are expected to exist in equal concentrations. Because of the localization of the unpaired electron in a σ orbital at the central carbon atom in **INT7a/b**, both structures are less stable than the resonance-stabilized 2-cyanoallylradcial **INT6** by about 100 kJ mol^{-1}. Similar to the methylacetylene reaction, both complexes **INT7b** and **INT6** are connected via a CN group migration through a cyclic intermediate **INT10**. This structure resides in a shallow potential energy minimum of 145 kJ mol^{-1} with respect to the separated reactants. **INT7a/b** can decay via final carbon−hydrogen bond

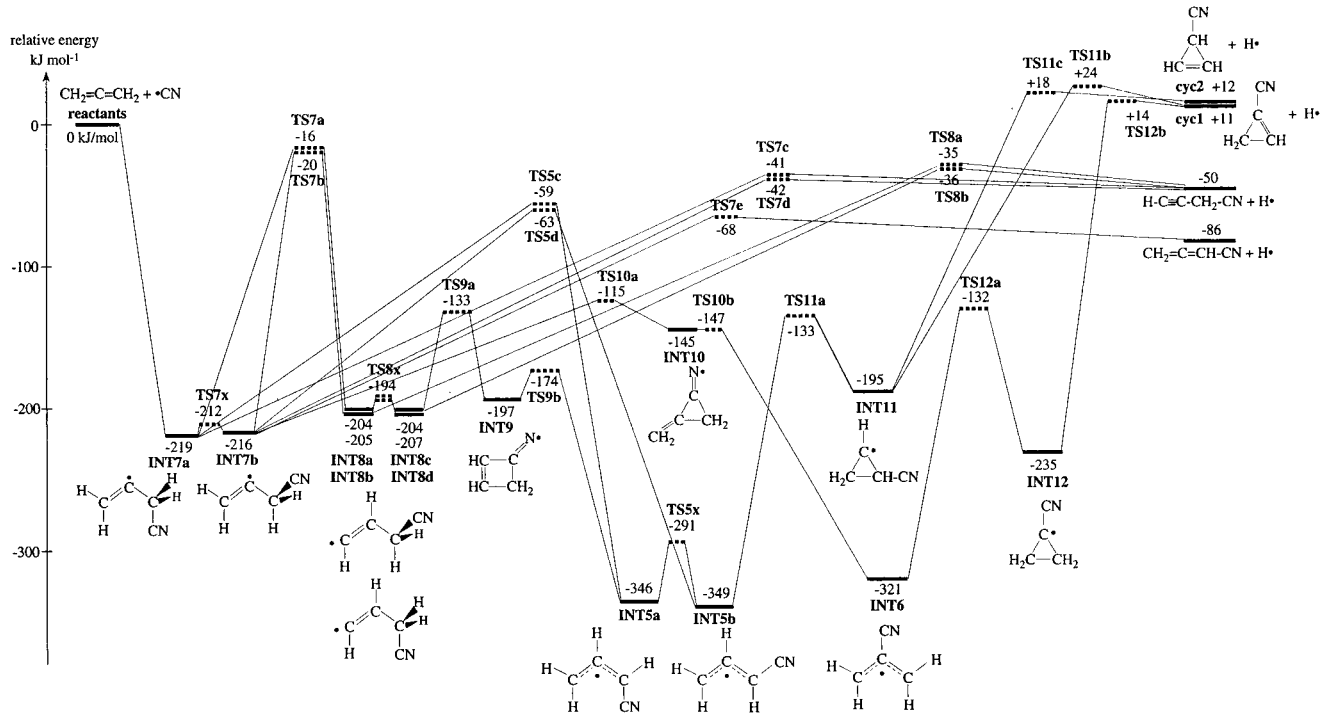

Figure 9. Schematic representation of the C_4H_3N potential energy surface of the CN + CH_2CCH_2 reaction. Only the most likely initial addition pathway is shown (see text).

ruptures to form cyanoallene $H_2CCCH(CN)$ or 3-cyanomethylacetylene $HCCCH_2CN$ through exit transition states **TS7e** and **TS7c/d** located 18 and 8−9 kJ mol^{-1} above the products.

Alternatively, **INT7a/b** can undergo a 1,2 H atom migration to form **INT5a/b** via **TS5c/d**. Both cyanoallyl structures **INT5a/b** and **INT6** can undergo ring closure to form cyclic intermediates **INT11** and **INT12** through **TS11a** and **TS12a**, respectively. A second pathway from **INT7a/b** to **INT5a/b** involves 3,2 H migrations to four distinct **INT8a/b/c/d** intermediates, followed by cyclization to **INT9**. In general, the intermediates **INT8a/b/c/d** and **INT9** are higher in energy than the open chain radicals because of their ring strengths. The energetically most favorable cyclic reaction products are 1-cyanocyclopropene (decomposition of **INT11** and **INT12**; **cyc1**) and 2-cyanocyclopropene (H atom loss from **INT11**; **cyc2**). However, the overall reaction energies are found to be endothermic by 11 and 12 kJ mol^{-1}, respectively. All exit transition states are located above the energy of the separated reactants.

B. Reaction Pathways. 1. Energetical Considerations. The high-energy cutoffs of the $P(E_T)$'s of the cyanoallene system are consistent with the formation of the cyanoallene isomer, $H_2CCCHCN$, in its $^1A'$ electronic ground state. The theoretically derived exothermicity of 86 kJ mol^{-1} falls within the experimentally derived range of 73−94 kJ mol^{-1}. Because the formation of 1- and 2-cyanocyclopropene molecules is endothermic by 11−12 kJ mol^{-1}, both isomers can likely be ruled out as a major reaction product. Here, the exit barriers from the decomposing intermediates **INT11** and **INT12** are located 14−24 kJ mol^{-1} above the energy of the separated reactants and can be passed only at our highest collision energy of 36.7 kJ mol^{-1}. Even if the electronic structure calculations overestimate the exit barriers by a few kJ mol^{-1}; hence, this pathway might be feasible at our highest collision energy, we emphasize that the experimental data at all three collision energies could be fit with basically the same $P(E_T)$, only that it is extended for the additional collision energy. Therefore, it is very likely that the less stable cyanocyclopropene isomers do not contribute significantly to our reactive scattering signal. This conclusion gains further support from the involved PES. **INT12** and **INT11** can be formed only via ring closures of **INT6** and **INT5b**. **INT6** would represent an initial addition complex if the cyano radical attacks the central carbon atom of the allene molecule. Because the reaction is dominated by large impact parameters, an addition to the central carbon atom is very unlikely, and **INT6** is likely only an unimportant intermediate. Rather, possible minor contributions of **INT6** will come from isomerization via **INT10** to **INT7b**, which in turn fragments via **TS7e** to the experimentally observed cyanoallene reaction product. This pathway involves lower barriers than does the **INT6** → **INT12** → 1-cyanopropene reaction sequence. **INT5a/b** can be excluded from the discussion as well because the high barrier of the H atom shift via **TS5c/d** would rather favor reaction to **INT10**. Summarizing, we can conclude that the cyanoallene isomer is the dominant reaction product. At present, however, minor contributions of the 3-cyanomethylacetylene isomer that is formed from the same decomposing complexes **INT7a/b** as is cyanoallene cannot be excluded.

Considering the reaction of methylacetylene with the cyano radicals, the crossed molecular beam studies clearly demonstrate the existence of a CN versus H atom exchange to C_4H_3N isomer(s). The experiment with CD_3CCH verifies further that both D and H atom losses form two distinct reaction products in a ratio of 1:1.[3a] The H atom-elimination pathway conserves the methyl group to form 1-cyanomethylacetylene, whereas the D loss underlines the synthesis of the cyanoallene isomer. The calculated reaction energies of 106 and 94 kJ mol^{-1} are well-covered by our experimental data, as derived from the center-of-mass translational-energy distributions. Let us finally comment on whether this reaction can form the cyanocyclopropene isomer. Because the formation of these structures is endothermic by about 19−20 kJ mol^{-1}, they cannot be synthesized at the lowest collision energy of 13.4 kJ mol^{-1}. Furthermore, taking into account the exit barriers of 3−12 kJ mol^{-1}, the minimum energy

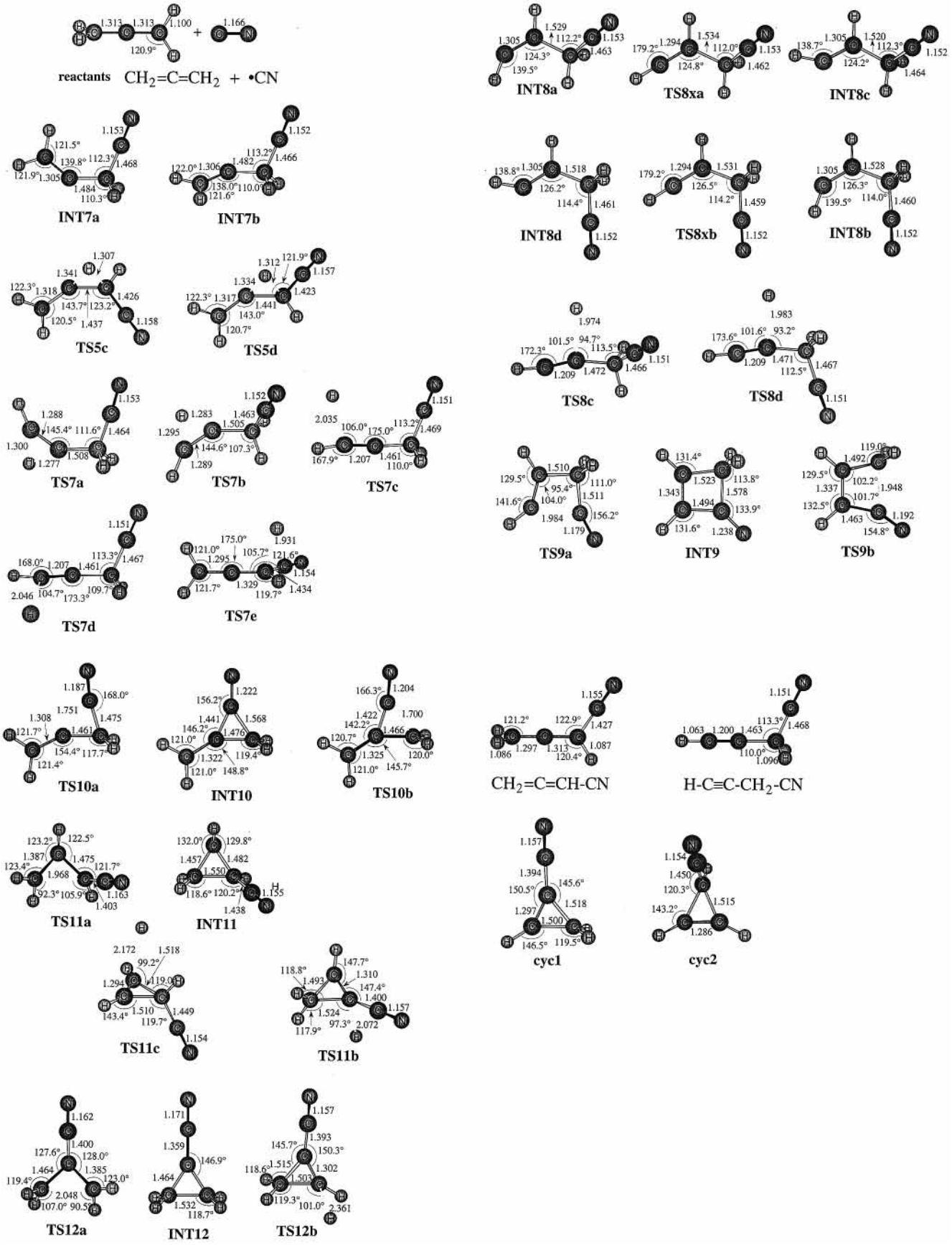

Figure 10. Important bond distances (Å) and bond angles (deg) of reactants, intermediates, transition states, and products of Figure 9.

required to open these channels is on the order of 22−32 kJ mol^{-1}. Because our highest collision energy was 34.9 kJ mol^{-1}, both isomers can likely be dismissed as major reaction products.

A closer look at the pertinent potential energy surface supports these conclusions. The existence of **INT5b** or **INT6** is crucial to the formation of 1- or 2-cyanocyclopropene. The latter can

be formed only via hydrogen migration from **INT2a**, but the high barrier of **TS6** compared to that of **TS3a/b** favors a CN group migration rather than a hydrogen shift and **INT6** cannot be formed in the reaction of cyano radicals with methylacetylene. Pathways to **INT5b** include multistep sequences **INT1a** → **INT4** → **INT5a** → **INT5b** and **INT1a** → **INT1b** → **INT5b**. All involved transition states lie at least 84−85 kJ mol^{-1} below the energy of the reactants. Because **TS4d** is lower than **TS4b**, any **INT4** would decompose to cyanoacetylene rather than undergo a hydrogen shift. However, cyanocyclopropene products might be minor contributors.

2. Angular Distribution Considerations. The forward−backward symmetric center-of-mass angular distributions of the allene systems and the lowest collision energy of the CN + CH_3CCH reaction indicate that the reaction proceeds through an indirect mechanism via the formation a complex with a lifetime longer than its rotation period. An alternative interpretation of a symmetric-exit transition state can be dismissed. In fact, on the basis of our potential energy surface, the only existing symmetric-exit transition state could arise from **INT6** to form 1-cyanocyclopropene. This intermediate, however, was found to play only a minor role in the chemical dynamics of the reaction. At both higher collision energies of 24.7 and 34.9 kJ mol^{-1}, the angular distributions of the methylacetylene reaction depict slightly forward scattering. This shape might suggest the occurrence of osculating C_4H_3N complexes (i.e., intermediates having lifetimes comparable to their rotational periods).

3. Actual Reaction Pathways. In this section, we describe the actual reaction pathways on the basis of our experimental and theoretical results. In the case of the CN($X^2\Sigma^+$) + CH_2-CCH_2 reaction, the CN radical attacks the carbon−carbon double bond of the allene molecule at the terminal carbon atom without the entrance barrier to form a carbon−carbon σ bond and a C_s symmetric *trans*-3-cyanopropen-1-yl-2 collision complex **INT7a** on the $^2A'$ surface, followed by a rapid trans−cis isomerization to **INT7b**. Because both structures are almost isoenergetic and **TS7x** is located only a few kJ mol^{-1} above **INT7a/b**, both isomers are expected to exist in equal amount. These H_2CCCH_2-(CN) intermediates resemble prolate asymmetric top radicals and are bound by 219 and 216 kJ mol^{-1} with respect to the reactants; these potential energy wells verify the experimentally found indirect collision dynamics via complex formation. All five heavy atoms are expected to rotate in a plane that is almost perpendicular to the total angular momentum vector **J** around the *C* axis. An initial attack on the central carbon atom of the allene molecule forming **INT6** can likely be ruled out. Although the latter is thermodynamically favored by about 100 kJ mol^{-1} compared to **INT7a/b**, the isotropic center-of-mass angular distributions and angular momentum conservation reveal that the reaction products are highly rotationally excited. Therefore, reactive trajectories should be dominated by large impact parameters to account for the rotational excitation. However, an addition to the central carbon atom of the allene molecule is supported only by small impact parameters close to zero. In the limiting case, this impact parameter value leads to a vanishing initial orbital angular momentum vector **L**; hence, no rotational excitation of the product isomers is expected. On the basis of the shapes of the $T(\theta)$'s, this result is clearly not observed experimentally, and **INT6** can likely be ruled out as a major reaction intermediate. Minor contributions are expected to undergo cyano group migrations via **INT10** to **INT7a/b**. Likewise, a hydrogen shift in the initial addition complexes **INT7a/b** was found to be only a minor pathway, if any. The fate of **INT7a/b** is two-fold. The reaction energy found experimentally strongly suggests the formation of the cyanoallene isomer. The relatively tight exit transition state **TS7e** located 18 kJ mol^{-1} above the separated products is supported by the $P(E_T)$'s peaking well away from zero translational energy (i.e., 27−50 kJ mol^{-1}). As outlined previously, minor contributions of the 3-cyanomethylacetylene from the decomposing **INT7a/b** intermediate via less tight exit transition states **TS7c/d** could not be ruled out. Preliminary statistical calculations reveal a cyanoallene versus 3-cyanocyanomethylacetylene ratio of about 9:1 and hence a dominant formation of the energetically more favorable isomer.[19]

Similar to that of the CN/allene system, the reaction of cyano radical with methylacetylene is dominated by a complex-forming reaction mechanism. Here, CN($X^2\Sigma^+$) adds barrierlessly to the C1 atom yielding **INT1a/b**, which are bound by about 250 kJ mol^{-1} with respect to the separated reactants. Because **TSx1** lies only ca. 17 kJ mol^{-1} above the initial trans and cis collision complexes, we expect equal concentrations of **INT1a** and **INT1b**. An addition to the C2 atom of the methylacetylene can be very likely ruled out as a dominant reaction pathway. First, the concept of regioselectivity of electrophilic radical attacks on unsaturated hydrocarbon molecules[20] predicts that the addition is directed to the carbon center that holds the highest electron density. Because partial delocalization of the methyl π-group orbitals increases the spin density at C1 at the expense of that at C2, the cyano radical preferentilly attacks the terminal carbon atom. Second, the sterical hindrance of the bulky methyl group reduces the cone of acceptance at C2 and hence the range of reactive impact parameters. Both effects together are suggested to direct the addition to C1, which is supported by recent low-temperature kinetic studies of this reaction[21] that has rate constants on the order of gas kinetics of $2-5 \times 10^{-10}$ cm^3 s^{-1}. Because this reaction proceeds without an entrance barrier and within orbiting limits, the overwhelming contribution of large impact parameters to the capture process is evident. However, if the cyano radical attacks C2, only low-impact parameters should dominate the reaction. Finally, these small impact parameters cannot account for the rotational excitation of the reaction products as found experimentally. In summary, all considerations suggest a predominant initial attack on the C1 atom of the methylacetylene molecule; only minor contributions from small impact parameters could form **INT2a/b**, which then isomerizes via **INT3** to **INT1a/b**. A competing hydrogen migration in **INT2a** to **INT6** can be ruled out, considering the much higher barrier. On the basis of our isotopic substitution experiments, the initial collision complexes are found to decay via two pathways. The dynamics of the first channel proceed via emission of the acetylenic hydrogen atom and maintenance of the methyl group to form 1-cyanomethylacetylene via **TS1c**. The second pathway, a carbon−hydrogen (deuterium in the CD_3-CCH experiment) bond rupture of the aliphatic bond at the methyl group via **TS1a/b**, forms cyanoallene, which indicates that the lifetime of the decomposing intermediates is long enough for the energy to flow from the activated carbon−carbon σ bond at the C1 to the breaking carbon−hydrogen bond of the methyl group to give the substituted allene product. Finally, we point out the milder sideways scattering, as evident from the CM distributions compared to those of the CN + C_2H_2 reaction studied earlier.[3] Here, the HCC−H bond angle was found to be 109.8°, and the H−CCN angle of ca. 92.8° was found to account for the sideways peaking. In the methylacetylene reaction, the C−H angles in the exit transition states are 94.5, 104.2, and 107.0°. These findings, together with energeti-

cally accessible C−H low-frequency bending and wagging modes, should be reflected in sideways peaking. However, the existence of a second reaction channel and the corresponding C−H bond rupture at the methyl group likely smears out the expected stronger sideways peaking, as found in the reaction of cyano radicals with acetylene.

C. Comparison with the $C_2D(^2\Sigma^+)$ + CH_3CCH Reaction. Both the CN and the C_2D radicals have a $^2\Sigma^+$ electronic ground state. Directed by the increased spin density at the C1 carbon atom of the methylacetylene and a screening effect of the CH_3 group, the radical adds barrierlessly to the π electron density to a new carbon−carbon σ bond to form CH_3CCHX (X = CN, C_2D).[10] Both reactions proceed via indirect scattering dynamics through complex formation; the initial addition complexes dwell in deep potential energy minima of about 253 (X = CN) and 267 kJ mol^{-1} (X = C_2D). But whereas the CN reaction goes through an oscillating complex at a collision energy of 24.7 kJ mol^{-1}, the C_2D/CH_3CCH system shows a long-lived CH_3CCHC_2D intermediate at a comparable collision energy, which could be explained in terms of an additional atom of the C_2D versus CN reactants (increasing the number of vibrational modes by three) and the low-frequency modes of the C−D wagging/bending vibrations in the range of 100−260 cm^{-1}. Furthermore, the lifetime of the decomposing intermediates in both systems is long enough for the energy to flow from the activated C−X bond at the C1 to the breaking C−H bond of the methyl group to give a substituted allene product. Therefore, the energy randomization in both CH_3CCHX intermediates is likely to be complete. Despite these similarities, one significant difference prevails. The branching ratio of the formation of $CH_3-C\equiv C-X$ versus H_2CCCHX is unity for X = CN but increases to 3−9 for X = C_2H based on our experiments. This increase might be the effect of a larger difference in the energetics of the exit transition states to both isomers in the C_2D case (22.3 kJ mol^{-1}) compared to the energetics of the CN/CH_3CCH reaction (1−2 kJ mol^{-1}) and hence larger unimolecular rate constants of the decomposing intermediates.

VI. Implications to Interstellar and Solar System Chemistry

Our crossed-beam experiments and electronic structure calculations have demonstrated for the very first time that C_4H_3N isomers can be synthesized in bimolecular collisions of cyano radicals, CN ($X^2\Sigma^+$), with allene and methylacetylene. All important reaction pathways are barrierless and exothermic, and all transition states involved are well below the energy of the separated reactants. Therefore, 1-cyanomethylacetylene, CH_3CCCN (X^1A_1), cyanoallene, $H_2CCCH(CN)$ (X^1A'), and 3-cyanomethylacetylene, $CH_2(CN)CCH$ (X^1A'), are expected to be present in low-temperature extraterrestrial environments such as cold molecular clouds and the atmosphere of Saturn's moon Titan. In both interstellar and planetary environments, the cyano radical is ubiquitous, as detected in the Taurus molecular cloud (TMC-1) and toward the Orion molecular cloud (OMC-1). Upon reactions with methylacetylene, for example, 1-cyanomethylacetylene as observed in TMC-1 is likely to be formed.[22] The versatile concept of a CN versus H exchange as established in our study makes it feasible to predict even the formation zones of nitriles in the ISM once the corresponding unsaturated hydrocarbons are identified in the interstellar medium. Because methylacetylene is the common precursor to $H_2CCCH(CN)$ and CH_3CCCN and because CH_3CCCN has been already assigned in TMC-1, $H_2CCCH(CN)$ is strongly expected to be present in TMC-1 as well. A search for this isomer is currently underway at the 100-m radio telescope in Effelsberg, Germany.[23] Various C_4H_3N reaction intermediates involved in both title reactions are irrelevant to the chemistry in cold molecular clouds because the number densities in these environments are too low to allow third-body stabilization. However, these doublet radicals should complement future chemical models of the denser atmospheres of the giant gas planets Jupiter, Saturn, Uranus, and Neptune as well as their moons Triton (Neptune) and Titan (Saturn). Here, encounters can divert the excess energy of the radical intermediates to stabilize them.

VII. Conclusions

Crossed molecular-beam reactions of cyano radicals, CN ($X^2\Sigma^+$), with allene, H_2CCCH_2 (X^1A_1), and methylacetylene, CH_3CCH (X^1A_1), have been investigated to elucidate the chemical reaction dynamics of the formation of C_4H_3N isomers under single-collision conditions. Our experimental results combined with electronic structure calculations show that both reactions have no entrance barrier, proceed via indirect, complex-forming reaction dynamics, and are initiated by addition of CN ($X^2\Sigma^+$) to the π electron density of the unsaturated hydrocarbon at the terminal carbon atom to form $CH_3CCH(CN)$ (methylacetylene reaction) and $H_2CCCH_2(CN)$ (allene reaction) intermediates on $^2A'$ surfaces. These complexes fragment via exit transition states located 8−19 kJ mol^{-1} above those of the products to form 1-cyanomethylacetylene, CH_3CCCN (X^1A_1), together with cyanoallene, $H_2CCCHCN$ (X^1A'), (ratio = 1:1; methylacetylene system) and 3-cyanomethylacetylene, $CH_2(CN)CCH$ (X^1A'), together with cyanoallene, $H_2CCCHCN$ (X^1A') (ratio = 1:9, allene system). A previous investigation suggested that the $CH_3CCH(CN)$ intermediate might undergo H atom migration to CH_3HCCCN to a small extent and that CH_3HCCCN then decomposes to 1-cyanomethylacetylene plus atomic hydrogen, cyanoacetylene, HCCCN ($X^1\Sigma^+$), and a methyl radical.[8)] Because both reactions are barrierless and exothermic and all of the involved exit transition states lie below the energy of the separated reactants, all hydrogen-deficient nitriles identified in our investigation can be synthesized in the atmosphere of Saturn's moon Titan and in molecular clouds at temperatures as low as 10 K.

Acknowledgment. R.-I.K is indebted the Deutsche Forschungsgemeinschaft (DFG) for a Habilitation fellowship (IIC1-Ka1081/3-1). Ab initio calculations were carried out at the computer center of the Institute for Molecular Science, Japan. This work was further supported by Academia Sinica. After September 2000, support from the University of York, United Kingdom, (R.-I.K) is gratefully acknowledged. Y.O. acknowledges partial support of the Grant-in-Aid from the Ministry of Education, Science, and Culture, Japan.

References and Notes

(1) (a) Cherchneff, I.; Glassgold, A. E. *Ap. J.* **1993**, 419, L41. (b) Millar, T. J.; Herbst, E. *Astron. Astrophys.* **1994**, *288*, 561. (c) Doty, S. D.; Leung, C. M. *Ap. J.* **1998**, *502*, 898.

(2) (a) Smith, I. W. M.; Sims, I. R.; Rowe, B. R. *Chem.—Eur. J.* **1997**, *3*, 1925. (b) Smith, I. W. M.; Rowe, B. R. *Acc. Chem. Res.* **2000**, *33*, 261.

(3) (a) Huang, L. C. L.; Lee, Y. T.; Kaiser, R. I. *J. Chem. Phys.* **1999**, *110*, 7119. (b) Huang, L. C. L.; Chang, A. H. H.; Asvany, O.; Balucani, N.; Lin, S. H.; Lee, Y. T.; Kaiser, R. I.; Osamura, Y. *J. Chem. Phys.* **2000**, *113*, 8656.

(4) Balucani, N.; Asvany, O.; Chang, A. H. H.; Lin, S. H.; Lee, Y. T.; Kaiser, R. I.; Bettinger, H. F.; Schleyer, P. v. R.; Schaefer, H. F. *J. Chem. Phys.* **1999**, *111*, 7457.

(5) Balucani, N.; Asvany, O.; Chang, A. H. H.; Lin, S. H.; Lee, Y. T.; Kaiser, R. I.; Bettinger, H. F.; Schleyer, P. v. R.; Schaefer, H. F. *J. Chem. Phys.* **1999**, *111*, 7472.

(6) Balucani, N.; Asvany, O.; Chang, A. H. H. Chang; Lin, S. H.; Lee, Y. T.; Kaiser, R. I.; Osamura, Y. *J. Chem. Phys.* **2000**, *113*, 8643.

(7) Huang, L. C. L.; Balucani, N.; Lee, Y. T.; Kaiser, R. I.; Osamura, Y. *J. Chem. Phys.* **199**, *111*, 2857.

(8) (a) Balucani, N.; Asvany, O.; Huang, L. C. L.; Lee, Y. T.; Kaiser, R. I.; Osamura, Y.; Bettinger, H. F. *Astrophys. J.* **2000**, *545*, 892. (b) Kaiser, R. I.; Balucani, N. *Acc. Chem. Res.* **2001**, *34*, 699.

(9) (a) Balucani, N.; Asvany, O.; Huang, L. C. L.; Lee, Y. T.; Kaiser, R. I.; Osamura, Y *Planet. Space Sci.* **2000**, *48*, 447. (b) Kaiser, R. I.; Balucani, N.; Asvany, O.; Lee, Y. T. In *Astrochemistry: From Molecular Clouds to Planetary Systems*; Mihn, Y. C., van Dishoek, E. F. Eds.; Astronomical Society of the Pacific Editions, IAU Series; 2000; Vol. 197, p 251.

(10) Kaiser, R. I.; Chiong, C. C.; Asvany, O.; Lee, Y. T.; Stahl, F.; Schleyer, P. v. R.; Schaefer, H. F. *J. Chem. Phys* **2001**, *114*, 3488. Stahl, F.; Schleyer, P. v. R.; Bettinger, H. F.; Kaiser, R. I.; Lee, Y. T.; Schaefer, H. F. *J. Chem. Phys.* **2001**, *114*, 3476.

(11) Lee, Y. T.; McDonald, J. D.; LeBreton, P. R.; Herschbach, D. R. *Rev. Sci. Instrum.* **1969**, *40*, 1402.

(12) Kaiser, R. I.; Ting, J.; Huang, L. C. L.; Balucani, N.; Asvany, O.; Lee, Y. T.; Chan, H.; Stranges, D.; Gee, D. *Rev. Sci. Instrum.* **1999**, *70*, 4185.

(13) Becke, A. D. *J. Chem. Phys.* **1992**, *97*, 9173.

(14) Lee, C.; Yang, W.; Parr, R. G. *Phys. Rev.* **1988**, *B37*, 785.

(15) Krishnan, R.; Frisch, M.; Pople, J. A. *J. Chem. Phys.* **1988**, *72*, 4244.

(16) Frisch, M. J.; Trucks, G. W.; Schlegel, H. B.; Scuseria, G. E.; Robb, M. A.; Cheeseman, J. R.; Zakrzewski, V. G.; Montgomery, J. A., Jr.; Stratmann, R. E.; Burant, J. C.; Dapprich, S.; Millam, J. M.; Daniels, A. D.; Kudin, K. N.; Strain, M. C.; Farkas, O.; Tomasi, J.; Barone, V.; Cossi, M.; Cammi, R.; Mennucci, B.; Pomelli, C.; Adamo, C.; Clifford, S.; Ochterski, J.; Petersson, G. A.; Ayala, P. Y.; Cui, Q.; Morokuma, K.; Malick, D. K.; Rabuck, A. D.; Raghavachari, K.; Foresman, J. B.; Cioslowski, J.; Ortiz, J. V.; Stefanov, B. B.; Liu, G.; Liashenko, A.; Piskorz, P.; Komaromi, I.; Gomperts, R.; Martin, R. L.; Fox, D. J.; Keith, T.; Al-Laham, M. A.; Peng, C. Y.; Nanayakkara, A.; Gonzalez, C.; Challacombe, M.; Gill, P. M. W.; Johnson, B. G.; Chen, W.; Wong, M. W.; Andres, J. L.; Head-Gordon, M.; Replogle, E. S.; Pople, J. A. *Gaussian 98*, revision D.4; Gaussian, Inc.: Pittsburgh, PA, 1998.

(17) Purvis, G. D.; Bartlett, R. J. *J. Chem. Phys.* **1982**, *76*, 1910.

(18) Kaiser, R. I.; Ochsenfeld, C.; Head-Gordon, M.; Lee, Y. T.; Suits, A. G. *Science* **1996**, *274*, 1508.

(19) Chang, A. H. H. Private communication. Methods employed in the calculations are fully described in Eyring, H.; Lin, S. H.; Lin, S. M. *Basic Chemical Kinetics*; Wiley & Sons: New York, 1980. Chang, A. H. H.; Mebel, A. M.; Yang, X. M.; Lin, S. H.; Lee, Y. T. *J. Chem. Phys.* **1998**, *109*, 2748.

(20) Shaik, S. S.; Canadell, E. *J. Am. Chem. Soc.* **1990**, *112*, 1446.

(21) Sims, I. R. Private communication. 2001.

(22) Broten, N. W. *Ap. J.* **1984**, *276*, L25.

(23) Chin, Y.; Lemme, C.; Kaiser, R. I. *Ap. J.* To be submitted in 2001.